

# Charged Higgs production at linear colliders in large extra dimensions

Qiang Li<sup>a</sup>, Chong Sheng Li<sup>a</sup><sup>y</sup>, Robert J. Oakes<sup>bz</sup>, and LiLin Yang<sup>ax</sup>

<sup>a</sup> Department of Physics, Peking University, Beijing 100871, China

<sup>b</sup> Department of Physics and Astronomy,  
Northwestern University, Evanston, IL 60208-3112, USA

(Dated: February 19, 2019)

## Abstract

In the minimal supersymmetric standard model (MSSM) with large extra dimensions (LED), we study the contributions of virtual Kaluza-Klein (KK) gravitons to MSSM charged Higgs production, especially in the two important production processes  $e^+ e^- \rightarrow H^+ H^-$  and  $e^+ e^- \rightarrow H^- tb$ , at future linear colliders (LC). We find that KK graviton effects can significantly modify these total cross sections and also their differential cross sections compared to their respective MSSM values and, therefore, can be used to probe the effective scale  $T$  up to several TeV. For example, at  $\sqrt{s} = 2 \text{ TeV}$ , the cross sections for  $e^+ e^- \rightarrow H^+ H^-$  and  $e^+ e^- \rightarrow H^- tb$  in the MSSM are  $7.4 \text{ fb}$  for  $m_H = 150 \text{ GeV}$  and  $0.003 \text{ fb}$  for  $m_H = 1.1 \text{ TeV}$  and  $\tan \beta = 40$ , while in SUSY LED they are  $12.1 \text{ fb}$  and  $0.01 \text{ fb}$ , respectively, for  $T = 4 \text{ TeV}$ .

PACS numbers: 11.10.Kk, 12.60.Jv, 14.80.Cp

---

<sup>x</sup> Electronics address: qlphy@pku.edu.cn

<sup>y</sup> Electronics address: csli@pku.edu.cn

<sup>z</sup> Electronics address: roakes@northwestern.edu

<sup>x</sup> Electronics address: llyang@pku.edu.cn

## I. INTRODUCTION

The idea that quantum gravity can appear at the TeV energy scale well below the Planck mass  $M_p = 1.2 \times 10^9$  GeV was proposed in the 1990's [1, 2, 3, 4, 5, 6]. The large extra dimensions (LED) model [1] introduced by Arkani-Hamed, Dimopoulos and Dvali has attracted much attention. It has been emphasized that the presence of large extra dimensions brings a new solution to the hierarchy problem, which can take the place of other mechanisms, for example, low-energy supersymmetry. It naturally becomes interesting to examine a scenario which combines SUSY and LED, since SUSY and extra dimensions are two important features of string theory [7]. This new possibility leads to different phenomenology than the usual LED scenario, which we explore here.

In the SUSY LED scenario, as in the LED scheme, the total space-time has  $D = 4 + 6$  dimensions. The Standard Model and SUSY particles live in the usual  $3 + 1$  dimensional space, while gravity can propagate in the additional  $6$ -dimensional space, which is assumed for simplicity to be compactified on the  $6$ -dimensional torus  $T^6$  with a common radius  $R$ . Then the 4-dimensional Planck scale  $M_p$  is no longer the relevant scale but is related to the fundamental scale  $M_s$  as follows [1, 8]:

$$M_p^2 = M_s^{+2} (2 \pi R)^6; \quad (1)$$

where  $M_s = 10$  TeV. According to Eq. (1), deviations from the usual Newtonian gravitational force law can be expected at distances smaller than  $R = 2 \times 10^{17} \times 10^{-32}$  cm [8]. For  $n = 2$ , LED is consistent with the current experiments [9] since gravitational forces are not yet well probed at distances less than about a millimeter (However for  $n = 2$ , there are constraints arising from, e.g., supernova cooling, which require  $M_s = 10 \times 100$  TeV if  $n = 28$  [10]).

SUSY LED can be tested at future high energy colliders. In SUSY LED, just as in LED, there exist KK towers of massive spin-2 gravitons and scalars which can interact with the SM and SUSY fields. There are two classes of effects that can probe LED: real graviton emission and virtual KK tower exchange.

At future linear colliders the search for one or more Higgs bosons will be a central task. In the Standard Model (SM), the Higgs boson mass is a free parameter with an upper bound of  $m_H = 600 \pm 800$  GeV [10]. Beyond the SM, the Minimal Supersymmetric Standard Model (MSSM), whose Higgs sector is a special case of the Two Higgs Doublet Model (2HDM) [11],

is of particular theoretical interest, and contains five physical Higgs bosons: two neutral CP-even bosons  $h^0$  and  $H^0$ , one neutral CP-odd boson  $A^0$ , and two charged bosons  $H^\pm$ . The  $h^0$  is the lightest, with a mass  $m_{h^0} = 140$  GeV, including the radiative corrections [2], and is a SM-like Higgs boson especially in the decoupling region ( $m_{A^0} \gg m_{Z^0}$ ). The other four are not SM-like and their discovery, particularly the charged Higgs bosons, would provide evidence for the MSSM. If the  $H^\pm$  bosons have mass  $m_{H^\pm} < m_t - m_b$ , they will be produced mainly through the  $t \bar{t} H^\pm$  decays of top quarks, which can be produced singly or in pairs at an  $e^+ e^-$  LC [13]. If there is sufficient center of mass energy available,  $\frac{p_T}{s} > 2m_H$ , then charged Higgs pair production,  $e^+ e^- \rightarrow H^+ H^-$ , will be the dominant production mechanism [13, 14]. However, if  $m_H > \max(m_t - m_b; \frac{p_T}{s}=2)$ , then  $H^\pm$  bosons can only be produced singly. And  $e^+ e^- \rightarrow H^\pm tb$  [15, 16] is one of the most important single charged Higgs production processes that can also be used to measure the relevant Yukawa couplings. Therefore, for this process, we will focus on the region where  $\frac{p_T}{s}=2 < m_H < \frac{p_T}{s} = m_t - m_b$ . For  $\frac{p_T}{s} = 500$  GeV (1000 GeV), this implies that  $250 < m_H < 320$  GeV ( $500 < m_H < 820$  GeV).

In the following we consider the contributions of virtual KK gravitons to the MSSM charged Higgs production, especially in the two important production processes  $e^+ e^- \rightarrow H^+ H^-$  and  $e^+ e^- \rightarrow H^\pm tb$  at future linear colliders. The presentation is organized as follows: In Sect. II we present the calculations. In Sect. III we give the numerical results and discuss them. Sect. IV contains a brief conclusion.

## II. ANALYTIC CALCULATIONS

In this section we derive the cross section for MSSM charged Higgs production. The MSSM diagrams, including the additional virtual KK gravitons ( $G^{(n)}$ ), which contribute to the processes  $e^+ e^- \rightarrow H^+ H^-$  and  $e^+ e^- \rightarrow H^\pm tb$  are presented in Figs. 1 and 2, respectively.

In the four dimensional description the interaction Lagrangian between the scattering fields and the KK gravitons ( $G^{(n)}$ ) or KK scalars ( $H^{(n)}$ ) is given by [17]

$$L_{int} = \frac{1}{M_p} \sum_n \frac{0}{G^{(n)} T} + \frac{1}{3} \frac{s}{n+2} \frac{3(n-1)}{n+2} H^{(n)} T^A ; \quad (2)$$

where  $n = (n_1; n_2; \dots; n)$  with  $n_i$ 's being integers,  $M_p = M_p = \frac{p}{8} = 2.4 \times 10^8$  GeV is the

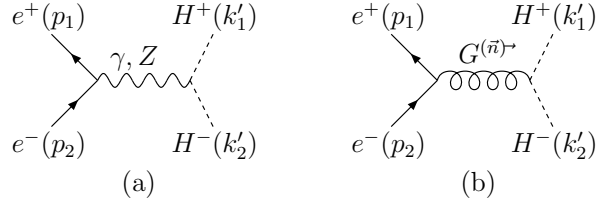


FIG .1: The M SSM Feynman diagrams and graviton mediated diagrams for  $e^+ e^- \rightarrow H^+ H^-$  at the tree level.

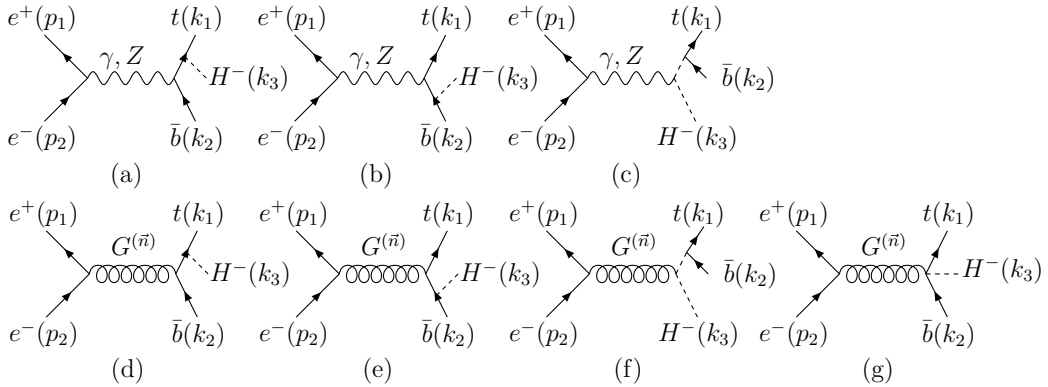


FIG .2: The M SSM Feynman diagrams and graviton mediated diagrams for  $e^+ e^- \rightarrow H tb$  at the tree level.

reduced four dimensional Planck scale, and  $T$  is the energy-momentum tensor of the scattering fields. The  $n$ -th KK mode graviton and scalar masses squared are both characterized by  $m_{(n)}^2 = j_n^2 = R^2$ . Since the trace of the energy-momentum tensor is proportional to the mass of the fields due to the field equations, we neglect processes mediated by the KK scalars in our study for the linear  $e^+ e^-$  collider, and consider only the processes mediated by the KK gravitons.

From Eq.(2) we can derive the relevant Feynman rules to be used in our calculations, which can be found in Ref. [17, 18]. The numerator of the graviton propagator  $P$  in the unitary gauge[17], is given by:

$$P = \frac{1}{2} + \frac{2}{3} + \dots; \quad (3)$$

where  $P$  is the Minkowski metric. The dots represent terms proportional to the graviton

momentum  $q$ , and since  $q \cdot T = 0$ , give a vanishing contribution to the amplitude. Note that the numerator of the graviton propagator in Ref. [18] is twice Eq. (3) and is the same as presented in Ref. [17]. However, the coupling constant squared in Ref. [17], i.e.,  $(\frac{p}{8} - M_p)^2$  in Eq. (2) is twice the one in Ref. [18]. Hence the results in the two references are consistent and we have been careful of this issue in our calculations.

We can write the amplitudes for the Feynman diagrams shown in Figs. 1 and 2 as follows:

$$\begin{aligned}
M_{1a} &= \frac{ie^2}{s} v(p_1) (\not{k}_2 - \not{k}_1) u(p_2) + \frac{ie^2 (c_w^2 - s_w^2)}{2(s - m_z^2) c_w^2 s_w^2} v(p_1) (\not{k}_2 - \not{k}_1) [(\frac{1}{2} - \frac{s_w^2}{c_w^2}) P_L - \frac{s_w^2}{c_w^2} P_R] u(p_2) \\
M_{1b} &= \frac{igP}{4} v(p_1) C u(p_2) \\
M_{2a} &= \frac{p}{3} \frac{ie^2 g}{2m_w s[(k_1 + k_3)^2 - m_b^2]} v(p_1) u(p_2) u(k_1; m_t) m_b \tan P_R + m_t \cot P_L \\
&\quad (k_1 + k_3 + m_b) v(k_2; m_b) + \\
&\quad \frac{p}{2m_w (s - m_z^2) c_w^2 s_w^2 [(k_1 + k_3)^2 - m_b^2]} v(p_1) [(\frac{1}{2} - \frac{s_w^2}{c_w^2}) P_L - \frac{s_w^2}{c_w^2} P_R] u(p_2) u(k_1; m_t) \\
&\quad m_b \tan P_R + m_t \cot P_L (k_1 + k_3 + m_b) [(\frac{1}{2} - \frac{1}{3} s_w^2) P_L - \frac{1}{3} s_w^2 P_R] v(k_2; m_b) \\
M_{2b} &= \frac{p}{3} \frac{2ie^2 g}{2m_w s[(k_2 + k_3)^2 - m_t^2]} v(p_1) u(p_2) u(k_1; m_t) (k_2 + k_3 - m_t) \\
&\quad m_b \tan P_R + m_t \cot P_L v(k_2; m_b) + \\
&\quad \frac{p}{2m_w (s - m_z^2) c_w^2 s_w^2 [(k_2 + k_3)^2 - m_t^2]} v(p_1) [(\frac{1}{2} - \frac{s_w^2}{c_w^2}) P_L - \frac{s_w^2}{c_w^2} P_R] u(p_2) u(k_1; m_t) \\
&\quad [(\frac{1}{2} - \frac{2}{3} s_w^2) P_L + \frac{2}{3} s_w^2 P_R] (k_2 + k_3 - m_t) m_b \tan P_R + m_t \cot P_L v(k_2; m_b) \\
M_{2c} &= \frac{p}{2m_w s[(k_1 + k_2)^2 - m_H^2]} v(p_1) (2 \not{k}_3 - \not{k}_1 - \not{k}_2) u(p_2) \\
&\quad u(k_1; m_t) m_b \tan P_R + m_t \cot P_L v(k_2; m_b) + \\
&\quad \frac{p}{2m_w (s - m_z^2) c_w^2 s_w^2 [(k_1 + k_2)^2 - m_H^2]} v(p_1) (2 \not{k}_3 - \not{k}_1 - \not{k}_2) [(\frac{1}{2} - \frac{s_w^2}{c_w^2}) P_L - \frac{s_w^2}{c_w^2} P_R] u(p_2) \\
&\quad u(k_1; m_t) m_b \tan P_R + m_t \cot P_L v(k_2; m_b) \\
M_{2d} &= \frac{igP}{16} \frac{p}{2m_w [(k_1 + k_3)^2 - m_b^2]} v(p_1) C u(p_2) \\
&\quad u(k_1; m_t) m_b \tan P_R + m_t \cot P_L (k_1 + k_3 + m_b)^b v(k_2; m_b) \\
M_{2e} &= \frac{igP}{16} \frac{p}{2m_w [(k_2 + k_3)^2 - m_t^2]} v(p_1) C u(p_2)
\end{aligned}$$

$$\begin{aligned}
u(k_1; m_t) & \stackrel{c}{=} (k_2 + k_3 - m_t) m_b \tan P_R + m_t \cot P_L v(k_2; m_b) \\
M_{2f} & = \frac{i g G P}{4 \frac{p}{2m_w} \frac{d}{[(k_1 + k_2)^2 - m_H^2]}} v(p_1) C u(p_2) \\
& u(k_1; m_t) m_b \tan P_R + m_t \cot P_L v(k_2; m_b) \\
M_{2g} & = 0
\end{aligned} \tag{4}$$

with

$$G = \frac{1}{M_p^2} \frac{1}{s - m_n^2} \tag{5}$$

$$C = [ (p_2 - p_1) + (\$) ] \tag{6}$$

$$a = m_H^2 (k_1^0 k_2^0) [ + ] \tag{7}$$

$$b = [ (k_1 + k_3 - k_2) (k_1 + k_3 - k_2 - 2m_b) ] + (\$) \tag{8}$$

$$c = [ (k_1 - k_3 - k_2) (k_1 - k_3 - k_2 - 2m_t) ] + (\$) \tag{9}$$

$$d = m_H^2 k_3 (k_1 + k_2) [ + ]; \tag{10}$$

where  $s = (p_1 + p_2)^2$ ,  $P_L = (1 - 5) = 2$ ,  $P_R = (1 + 5) = 2$ ,  $s_w = \sin_w$ ,  $c_w = \cos_w$  and  $\tan$  is the ratio of the two vacuum expectation values in the MSSM. Note that the contribution from Feynman diagram Fig 2 (g) vanishes since the trace of the graviton appears in this diagram and, therefore, in the limit of vanishing electron mass, this contribution also vanishes [19].

$G$  in Eq. (5) represents the summation of the KK excitation propagators. If the summation over the infinite tower of the KK modes is performed, one will encounter ultraviolet divergences. This happens because LED is an effective theory, which is only valid below an effective energy scale. In the following calculations we naively introduce an ultraviolet cutoff for the highest KK modes and replace the summation by [17]

$$\frac{4}{T} = \frac{1}{M_p^2} \frac{1}{s - m_n^2}; \tag{11}$$

where  $T$  is a cutoff scale naturally being of the order of the fundamental scale  $M_s$ .

Finally, the cross sections for the charged Higgs production processes in SUSY LED following from the amplitudes are:

$$(e^+ e^- \rightarrow H^+ H^-) = \frac{1}{2s} \frac{Z}{4} d \frac{1}{2} M_{1a} + M_{1b} \frac{f}{f} \tag{12}$$

$$(e^+ e^- \rightarrow H^+ tb) = \frac{1}{2s} d \frac{3}{4} M_{2a} + M_{2b} + M_{2c} + M_{2d} + M_{2e} + M_{2f} + M_{2g} \frac{f}{f}; \tag{13}$$

and the final state phase space hypercube elements are defined as

$$d_2 = \frac{0}{(2)^3 2k_i^0} \frac{Y^2}{A} \frac{1}{(2)^4} \frac{p_1 + p_2}{x^2} \frac{!}{k_j^0} ; \quad (14)$$

$$d_3 = \frac{0}{(2)^3 2k_i^0} \frac{Y^3}{A} \frac{1}{(2)^4} \frac{p_1 + p_2}{x^3} \frac{!}{k_j^0} ; \quad (15)$$

### III. NUMERICAL RESULTS

In the numerical calculations, we used the following set of SM parameters[20]:

$$m_w (m_w) = 128; m_w = 80.419 \text{ GeV}; m_t = 178 \text{ GeV}; m_z = 91.1882 \text{ GeV}; \quad (16)$$

For the Yukawa coupling of the bottom quark at the H tb vertex, as suggested by Ref.[16], we used the top quark pole mass and the QCD improved running mass  $m_b(Q)$  with  $m_b(m_b) = 4.25 \text{ GeV}$ , which were evaluated using the NLO formula [21] as follows:

$$m_b(Q) = U_f(Q; m_t) U_5(m_t; m_b) m_b(m_b); \quad (17)$$

Here the evolution factor  $U_f$  is

$$U_f(Q_2; Q_1) = \frac{s(Q_2)}{s(Q_1)} \frac{d^{(f)}}{1 + \frac{s(Q_1)}{4} \frac{s(Q_2)}{J^{(f)}}};$$

$$d^{(f)} = \frac{12}{33 - 2f}; \quad J^{(f)} = \frac{8982 - 504f + 40f^2}{3(33 - 2f)^2}; \quad (18)$$

and  $f$  is the number of active light quarks. For the energy scale  $Q$ , we chose  $Q = \sqrt{\frac{p_t}{m_t m_b m_H}}$  as in Ref. [16] for  $e^+ e^- \rightarrow H^- tb$ .

A.  $e^+ e^- \rightarrow H^- H^+$

In Figs. 3 and 4 we show the dependence of the cross sections in MSSM and SUSY LED for the process  $e^+ e^- \rightarrow H^- H^+$  on  $m_H$  assuming  $\sqrt{s} = 1000 \text{ GeV}$  and  $\sqrt{s} = 500 \text{ GeV}$ , respectively. The dashed lines represent the MSSM results and the solid lines represent the cross section in SUSY LED for different values of  $m_t$ . From the figures one can see that when  $\sqrt{s}$  is large ( $> 1 \text{ TeV}$ ) and  $m_H$  is small ( $< 400 \text{ GeV}$ ) the LED effects can be very large up to  $m_t = 2 \text{ TeV}$ . For example, when  $\sqrt{s} = 1 \text{ TeV}$  and  $m_H = 200 \text{ GeV}$  the cross section

in the M SSM is  $23.8 \text{ fb}$ , while for SUSY LED it is  $152.4 \text{ fb}$  for  $T = 1.5 \text{ TeV}$  and  $36.6 \text{ fb}$  for  $T = 2 \text{ TeV}$ .

In Fig. 5, the cross section in the M SSM and SUSY LED for the process  $e^+ e^- \rightarrow H^+ H^-$  are plotted as functions of  $\sqrt{s}$  assuming  $m_H = 200 \text{ GeV}$ . From this figure we see that the effects of virtual graviton exchange can substantially modify the  $e^+ e^- \rightarrow H^+ H^-$  cross section compared to its M SSM value, especially at large  $\sqrt{s} (> 4 \text{ TeV})$ , enabling LED up to  $T = 8 \text{ TeV}$  to be probed.

In Fig. 6 we show the dependence of the cross sections in the M SSM and SUSY LED for the process  $e^+ e^- \rightarrow H^+ H^-$  on the effective energy scale  $T$  assuming  $m_H = 150 \text{ GeV}$  and  $\sqrt{s} = 1000 \text{ GeV}$ ,  $2000 \text{ GeV}$ , and  $3000 \text{ GeV}$ . As expected, when  $\sqrt{s}$  is fixed the cross section in SUSY LED tends to the value in the M SSM when  $T$  tends becomes very large. In addition, the figure also shows that for large  $\sqrt{s}$  and small  $T$  the LED effects are very large. For example, for  $\sqrt{s} = 3 \text{ TeV}$  and  $T = 4 \text{ TeV}$  the cross section in the M SSM is  $3.4 \text{ fb}$  while the value in SUSY LED is  $58.7 \text{ fb}$ .

In Figs. 7 and 8, we present the differential cross section  $d\sigma/d\cos\theta$  in the M SSM and SUSY LED for the process  $e^+ e^- \rightarrow H^+ H^-$  as a function of  $\cos\theta$ , where the scattering angle  $\theta$  is the angle between  $H^+$  and the incoming positron assuming  $m_H = 200 \text{ GeV}$  and  $\sqrt{s} = 1000 \text{ GeV}$ , and  $T = 2000 \text{ GeV}$  and  $4000 \text{ GeV}$ , respectively. Both differential cross sections in the M SSM and SUSY LED vanish at  $\cos\theta = \pm 1$ . However, their shapes are different. Note that the LED cross section is not symmetric under  $\cos\theta \rightarrow -\cos\theta$  while the M SSM one is symmetric. We further have plotted the differential contributions to the SUSY LED cross section and find the asymmetry comes from the interference of the SUSY LED and M SSM amplitudes, which is in proportion to  $(t-u)(tu-m_H^4) = \frac{2}{T}(t-u)$  (where  $t$  and  $u$  are Mandelstam variables) and thus to  $\cos\theta \sin^2\theta$ . Moreover, the SUSY LED contribution has peaks in both the forward and backward regions and also vanishes at three points:  $\cos\theta = 0$  and  $\pm 1$ , as found in Ref. [22], since it is proportional to  $(t-u)^2(tu-m_H^4) = \frac{4}{T}$  and thus to  $\cos^2\theta \sin^2\theta$ .

## B. $e^+ e^- \rightarrow H^- tb$

In Figs. 9 and 10, we show the dependence of the cross section in the M SSM and SUSY LED for the process  $e^+ e^- \rightarrow H^- tb$  on  $m_H$  assuming  $\sqrt{s} = 1000 \text{ GeV}$  for  $\tan\beta = 40$

and  $\tan \beta = 10$ , respectively. The dashed lines represent the M SSM results and the solid lines represent the cross sections for SUSY LED with different values of  $\tan \beta$ . This figure shows that when  $\tan \beta = 2$  is small( $< 2.5$  TeV) and  $m_H$  is also small( $< 600$  GeV), the LED effects are very large. For example, when  $\tan \beta = 40$  and  $m_H = 550$  GeV the cross section in the M SSM is  $0.017$  fb, while for SUSY LED it is  $0.17$  fb for  $\tan \beta = 1.5$  TeV and  $0.02$  fb for  $\tan \beta = 2$  TeV.

In Figs. 11 and 12, we present the dependence of the cross section in the M SSM and for SUSY LED for the process  $e^+ e^- \rightarrow H \bar{t} b$  on  $\tan \beta$  assuming  $\sqrt{s} = 1000$  GeV and  $m_H = 520$  GeV in Fig. 11 and  $\sqrt{s} = 500$  GeV and  $m_H = 260$  GeV in Fig. 12. Observe that the cross section in both the M SSM and SUSY LED exhibit a close to  $\tan \beta$   $\frac{m_t m_b}{m_t^2 \cot^2 \beta + m_b^2 \tan^2 \beta} \approx 6$ , since the average strength of the  $\bar{t} b H$  coupling, which is proportional to  $\frac{m_t m_b}{m_t^2 \cot^2 \beta + m_b^2 \tan^2 \beta}$ , is then minimal [23]. From these figures one also sees that when  $\tan \beta = 2$  is small( $< 2.5$  TeV) and  $m_H$  is also small( $< 600$  GeV) the LED effects are large for  $\sqrt{s} = 1$  TeV. For  $\sqrt{s} = 0.5$  TeV the LED effects are only significant at small  $\tan \beta$  ( $< 1.5$  TeV) and large or small  $\tan \beta$ .

In Fig. 13 the cross sections in the M SSM and SUSY LED for the process  $e^+ e^- \rightarrow H \bar{t} b$  are plotted as functions of  $\sqrt{s}$ , assuming  $m_H = 800$  GeV and  $\tan \beta = 40$ . Since we are interested in the case where  $\sqrt{s} = 2 < m_H < \sqrt{s} = m_t = m_b$ ,  $\sqrt{s}$  should be in the range from about 983 GeV to 1600 GeV. From this figure we see that, as in the case of  $e^+ e^- \rightarrow H^+ H^-$ , the effects of virtual graviton exchange can significantly modify the  $e^+ e^- \rightarrow H \bar{t} b$  cross section compared to its M SSM value, especially at large  $\sqrt{s} (> 1.5$  TeV), where LED up to about  $\tan \beta = 3.5$  TeV can be probed.

In Fig. 14 we show the dependence of the cross section in the M SSM and SUSY LED for the process  $e^+ e^- \rightarrow H \bar{t} b$  on the effective energy scale  $\tan \beta$  assuming  $m_H = 260, 550$ , and  $1100$  GeV, and  $\sqrt{s} = 500, 1000$ , and  $2000$  GeV, respectively. As expected, when  $\sqrt{s}$  is fixed the SUSY LED cross section tends to the value in the M SSM when  $\tan \beta$  becomes very large. This figure also shows that for large  $\sqrt{s}$  and small  $\tan \beta$  the LED effects can be very large. For example, when  $\sqrt{s} = 2$  TeV and  $\tan \beta = 4$  TeV the cross section in the M SSM is  $0.006$  fb, while in SUSY LED it is  $0.013$  fb.

In Fig. 15 we show the differential cross sections  $d\sigma/dP_T(H)$  in the M SSM and SUSY LED for the process  $e^+ e^- \rightarrow H \bar{t} b$  as functions of the transverse momentum of the charged Higgs boson  $P_T$  assuming  $m_H = 520$  GeV,  $\sqrt{s} = 1000$  GeV, and  $\tan \beta = 1500, 2000$  GeV,

2500 GeV and 3000 GeV. The shape of the differential cross sections in the MSSM and for SUSY LED are slightly different. The LED effects generally enhance the differential cross sections, especially when  $T$  is small.

#### IV . SUM M A R Y

In the MSSM with large extra dimensions we investigated the contributions of virtual KK gravitons for the MSSM charged Higgs production in the two important production processes:  $e^+ e^- \rightarrow H^+ H^-$  and  $e^+ e^- \rightarrow H^- tb$  at future linear colliders. We found that KK gravitons can significantly modify these total cross sections and their differential cross sections compared to the corresponding MSSM values and, therefore, can be used to probe the effective scale  $T$  up to several TeV. For example, at  $\sqrt{s} = 2 \text{ TeV}$  the cross sections for  $e^+ e^- \rightarrow H^+ H^-$  and  $e^+ e^- \rightarrow H^- tb$  in the MSSM are  $7.4 \text{ fb}$  for  $m_H = 150 \text{ GeV}$  and  $0.006 \text{ fb}$  for  $m_H = 1.1 \text{ TeV}$  with  $\tan \beta = 40$ , while in SUSY LED they are  $12.1 \text{ fb}$  and  $0.013 \text{ fb}$ , respectively, for  $T = 4 \text{ TeV}$ .

#### Acknowledgments

We thank Prasanta Kumar Das for useful discussions. This work was supported by the National Natural Science Foundation of China and the Specialized Research Fund for the Doctoral Program of Higher Education and the U.S. Department of Energy, Division of High Energy Physics, under Grant No D E-FG 02-91-ER 4086.

---

- [1] N. Arkani-Hamed et al., *Phys.Lett.B* 429 (1998) 263; N. Arkani-Hamed et al., *Phys.Rev.D* 59 (1999) 086004; N. Arkani-Hamed et al., *Phys.Lett.B* 436 (1998) 257.
- [2] L. Randall, R. Sundrum, *Phys.Rev.Lett.* 83 (1999) 3370; L. Randall, R. Sundrum, *Phys.Rev.Lett.* 83 (1999) 4690.
- [3] J. Lykken, *Phys.Rev.D* 54 (1996) 3693.
- [4] E. Witten, *Nucl.Phys.B* 471 (1996) 135.
- [5] P. Horava and E. Witten, *Nucl.Phys.B* 460 (1996) 506; *Nucl.Phys.B* 475 (1996) 94.
- [6] I. Antoniadis, *Phys.Lett.B* 246 (1990) 377.

[7] J. Polchinski, *String Theory*, Cambridge University Press (2005).

[8] C. C. Saki, TASI Lectures on Extra Dimensions and Branes, [hep-ph/0404096](#).

[9] E. G. Adelberger [Eot-Wash Group Collaboration] [hep-ex/0202008](#).

[10] T. Hambye and K. Riesemann, *Phys. Rev. D* 55 (1997) 7255.

[11] H. E. Haber and G. L. Kane, *Phys. Rep.* 117 (1985) 75.

[12] H. E. Haber and R. Hempking, *Phys. Rev. Lett.* 66 (1991) 1815; Y. Okada et al., *Prog. Theor. Phys.* 85 (1991) 1; J. Ellis et al., *Phys. Lett. B* 257 (1991) 83; S. Heinemeyer, [hep-ph/0407244](#).

[13] S. Komamiya, *Phys. Rev. D* 38 (1988) 2158; J. Guasch et al., *Nucl. Phys. B* 596 (2001) 66.

[14] A. Arhrib and G. M. D'Olteka, *Nucl. Phys. B* 558 (1999) 3.

[15] S. Kanemura et al., *JHEP* 0102 (2001) 011; A. Djouadi et al., *Z. Phys. C* 54 (1992) 255.

[16] B. A. Kniehl et al., *Phys. Rev. D* 66 (2002) 054016.

[17] G. F. Giudice et al., *Nucl. Phys. B* 544 (1999) 3.

[18] T. Han, J. D. Lykken and R. J. Zhang, *Phys. Rev. D* 59 (1999) 105006.

[19] D. Choudhury, N. G. Deshpande, D. K. Ghosh, *JHEP* 0409 (2004) 055.

[20] Particle Data Group, S. Eidelman et al., *Phys. Lett. B* 592 (2004) 1.

[21] M. Carena et al., *Nucl. Phys. B* 577 (2000) 88.

[22] N. Delerue et al., *Phys. Rev. D* 70 (2004) 091701.

[23] A. Krause et al., *Nucl. Phys. B* 519 (1998) 85.

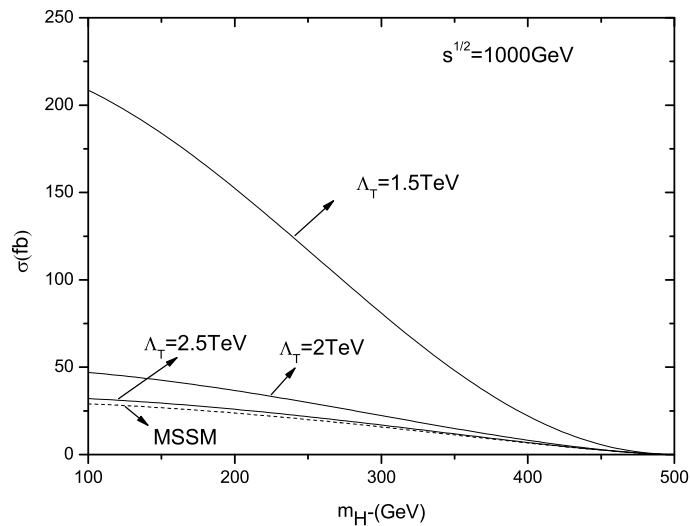


FIG . 3: D ependence of the cross section in the M SSM and SU SY LED for the process  $e^+ e^- \rightarrow H^+ H^-$  on  $m_H$  , assum ing  $\sqrt{s} = 1000 \text{ GeV}$  .

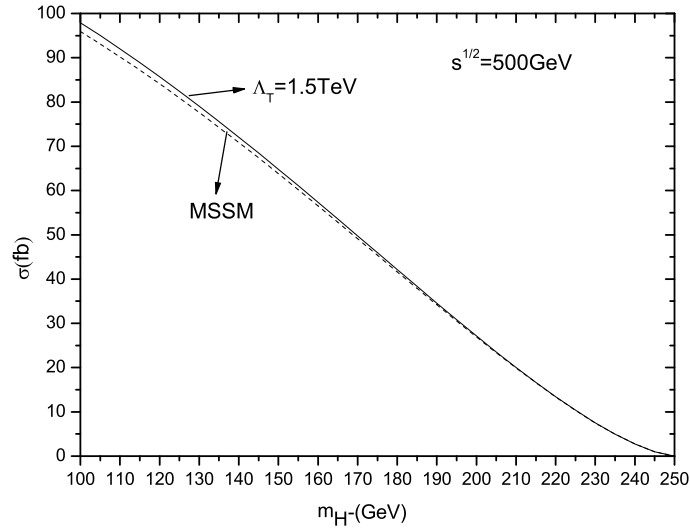


FIG . 4: D ependence of the cross section in the M SSM and SU SY LED for the process  $e^+ e^- \rightarrow H^+ H^-$  on  $m_H$  , assum ing  $\sqrt{s} = 500 \text{ GeV}$  .

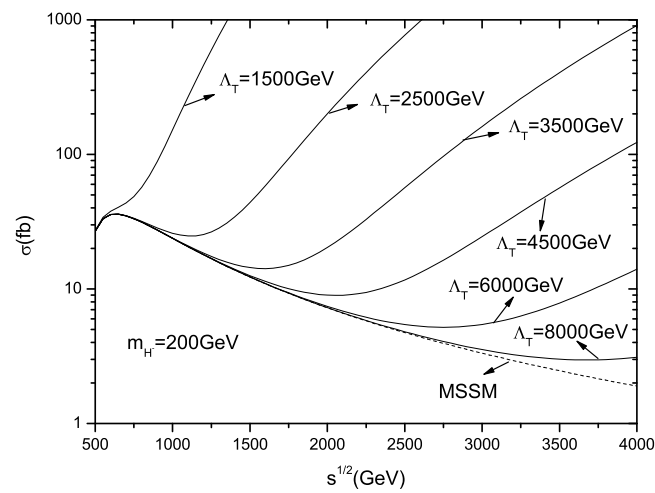


FIG . 5: D ependence of the cross section in the M SSM and SU SY LED for the process  $e^+ e^- \rightarrow H^+ H^-$  on  $\sqrt{s}$  , assum ing  $m_H = 200 \text{ GeV}$  .

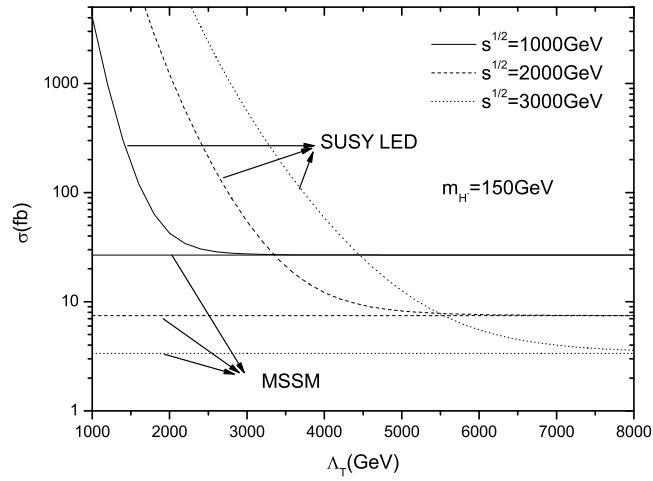


FIG . 6: D ependence of the cross section in the M SSM and SU SY LED for the process  $e^+ e^- \rightarrow H^+ H^-$  on the effective energy scale  $\Lambda_T$ , assuming  $m_H = 150$  GeV,  $\sqrt{s} = 1000$  GeV, 2000 GeV, and 3000 GeV .

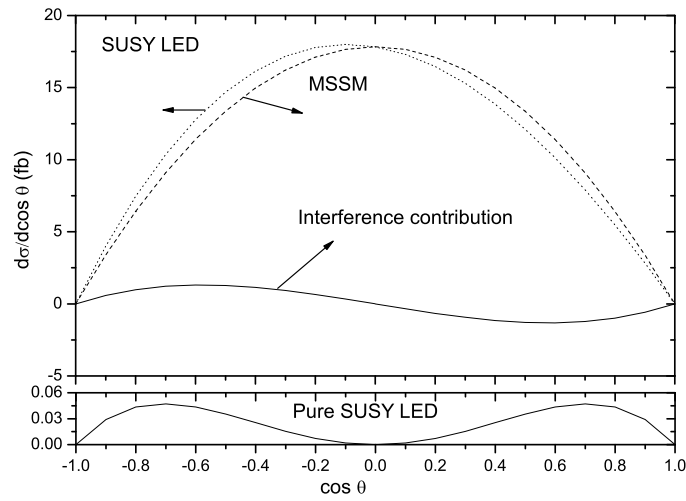


FIG . 7: The differential cross section  $d\sigma/d\cos\theta$  in the M SSM and SU SY LED for the process  $e^+ e^- \rightarrow H^+ H^-$  as functions of  $\cos\theta$ , assuming  $m_H = 200$  GeV,  $\sqrt{s} = 1000$  GeV,  $\Lambda_T = 4000$  GeV .

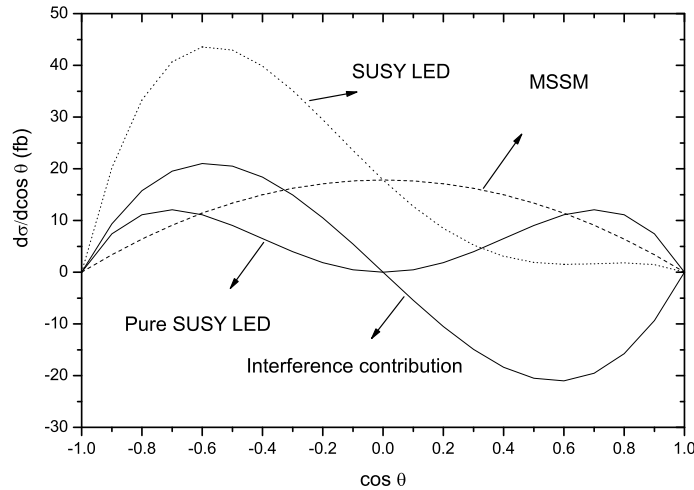


FIG. 8: The differential cross section  $d\sigma/d\cos\theta$  in the MSSM and SUSY LED for the process  $e^+ e^- \rightarrow H^+ H^-$  as functions of  $\cos\theta$ , assuming  $m_H = 200$  GeV,  $\sqrt{s} = 1000$  GeV,  $\tan\beta = 2000$  GeV.

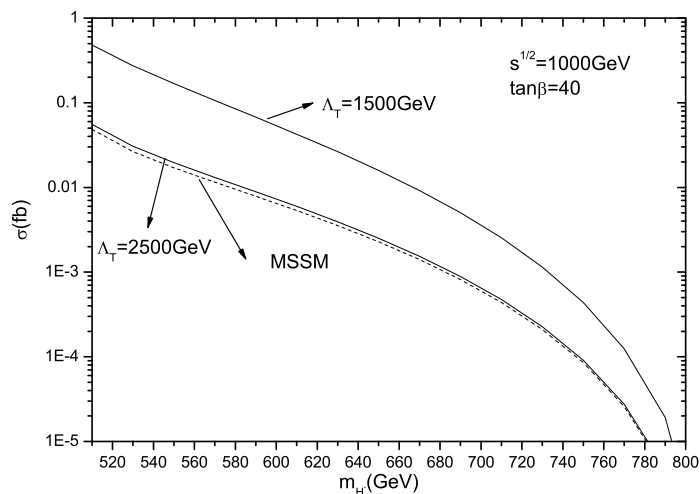


FIG. 9: Dependence of the cross section in the MSSM and SUSY LED for the process  $e^+ e^- \rightarrow H^+ H^-$  on  $m_H$ , assuming  $\sqrt{s} = 1000$  GeV,  $\tan\beta = 40$ .

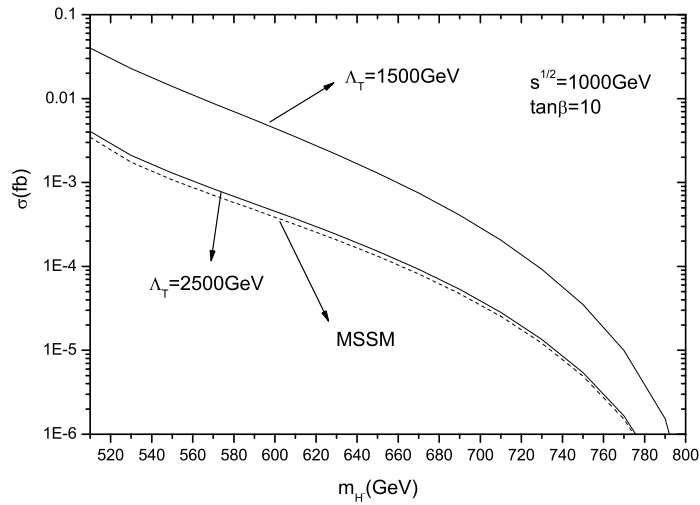


FIG .10: D ependence of the cross section in the M SSM and SU SY LED for the process  $e^+ e^- \rightarrow H$  tb on  $m_H$  , assum ing  $\frac{p_T}{s} = 1000 \text{ GeV}$  ,  $\tan \beta = 10$  .

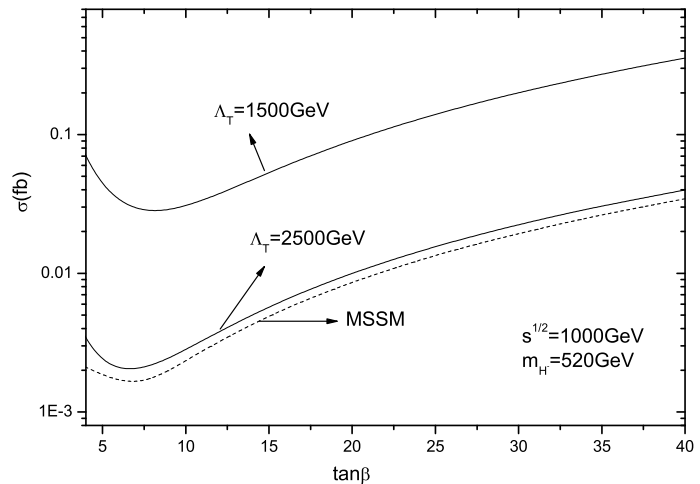


FIG .11: D ependence of the cross section in the M SSM and SU SY LED for the process  $e^+ e^- \rightarrow H$  tb on  $\tan \beta$  , assum ing  $\frac{p_T}{s} = 1000 \text{ GeV}$  ,  $m_H = 520 \text{ GeV}$  .

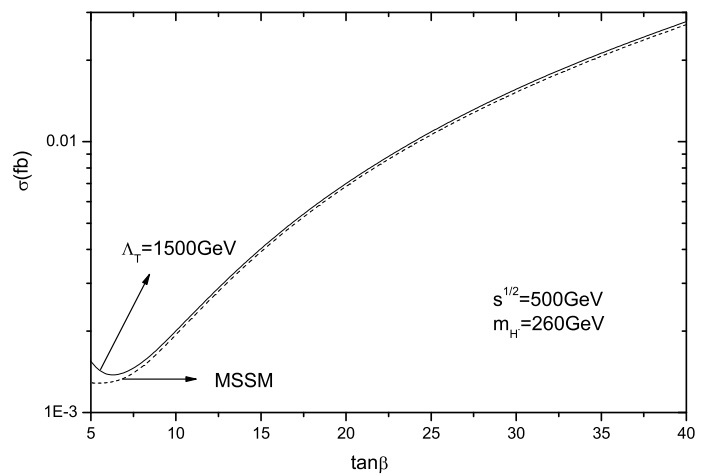


FIG. 12: Dependence of the cross section in the MSSM and SUSY LED for the process  $e^+ e^- \rightarrow H$  on  $\tan\beta$ , assuming  $\sqrt{s} = 500$  GeV,  $m_H = 260$  GeV.

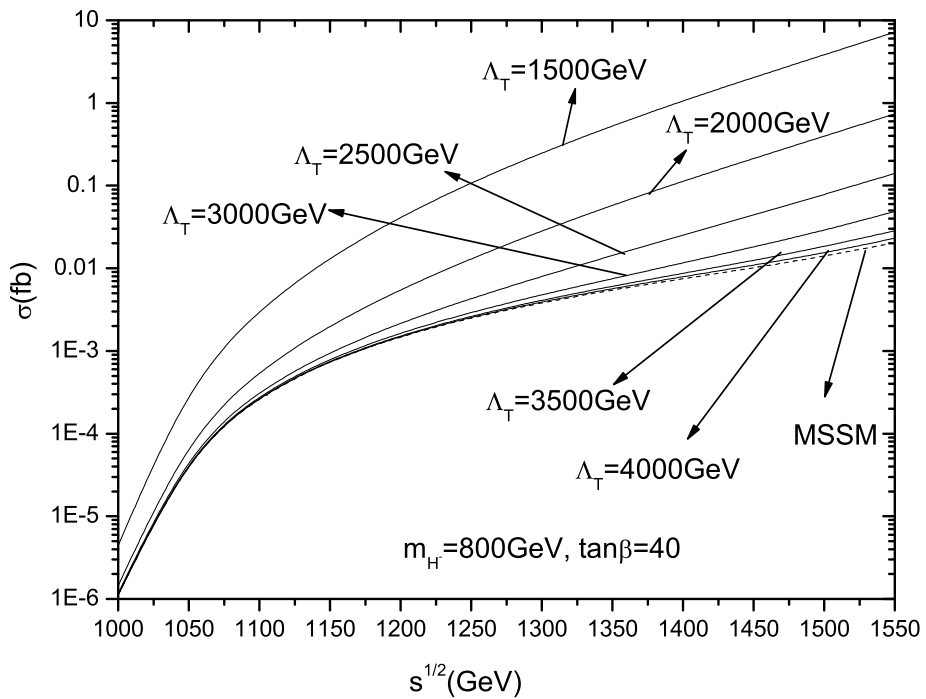


FIG . 13: D ependence of the cross section in the M SSM and SUSY LED for the process  $e^+ e^- \rightarrow H$  to on  $\frac{p}{s}$ , assuming  $m_H = 800$  GeV,  $\tan \beta = 40$ .

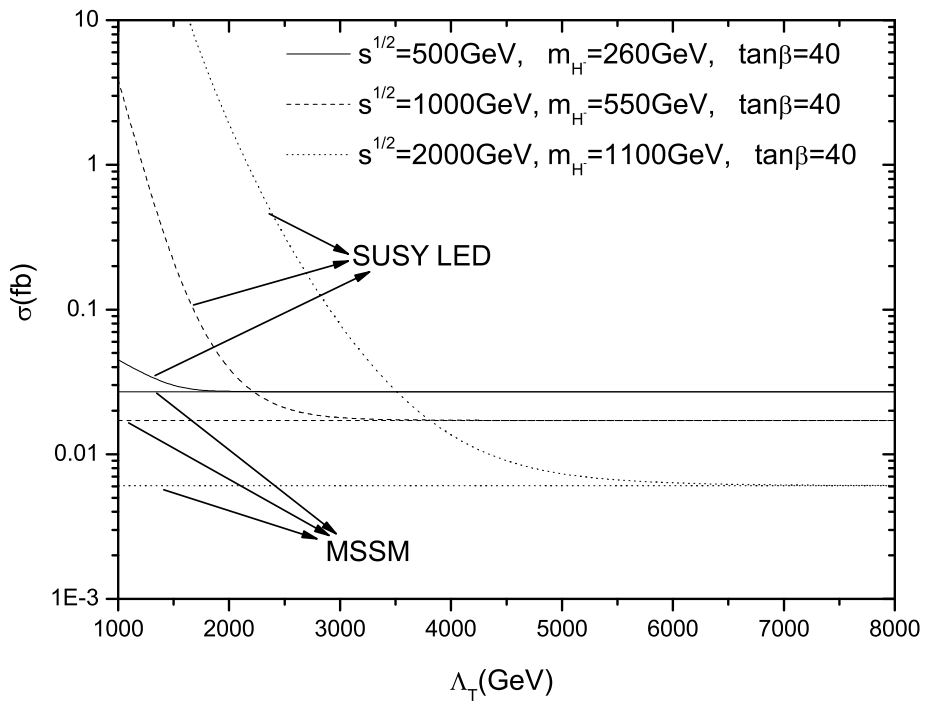


FIG. 14: Dependence of the cross section in the MSSM and SUSY LED for the process  $e^+ e^- \rightarrow H tb$  on the effective energy scale  $\Lambda_T$ , assuming  $m_H = 260; 550; 1100$  GeV, and  $\sqrt{s} = 500; 1000; 2000$  GeV, respectively.

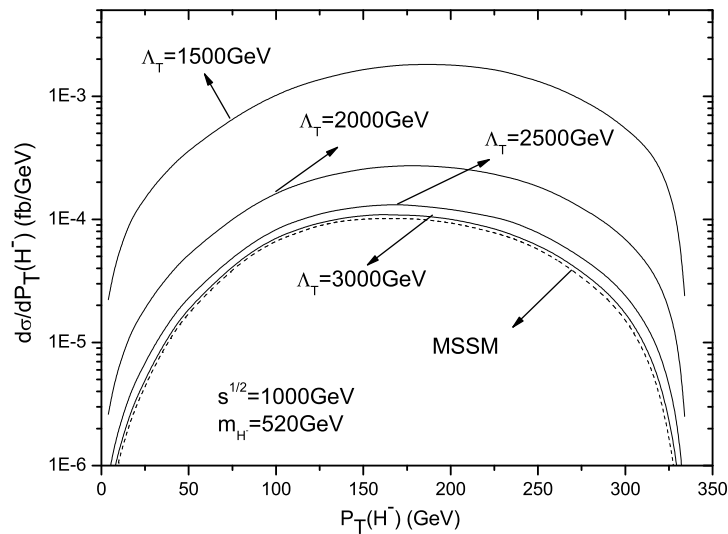


FIG. 15: The differential cross section  $d\sigma/dP_T(H^-)$  in the MSSM and SUSY LED for the process  $e^+ e^- \rightarrow H^-$  as a function of the transverse momentum of the charged Higgs boson  $P_T$ , assuming  $m_{H^-} = 520 \text{ GeV}$ ,  $\sqrt{s} = 1000 \text{ GeV}$ ,  $\Lambda_T = 1500 \text{ GeV}, 2000 \text{ GeV}, 2500 \text{ GeV}$  and  $3000 \text{ GeV}$ .